*Article*

# Ionic Strength Effect in the Equilibrium and Rheological Behavior of an Amphiphilic Triblock Copolymer at the Air/Solution Interface

Carlo Carbone [1], Eduardo Guzmán [1,2,*], Julia Maldonado-Valderrama [3], Ramón G. Rubio [1,2] and Francisco Ortega [1,2,*]

1 Departamento de Química Física, Facultad de Ciencias Químicas, Universidad Complutense de Madrid, Plaza de las Ciencias 2, Ciudad Universitaria, 28040 Madrid, Spain; carlcarb@ucm.es (C.C.); rgrubio@quim.ucm.es (R.G.R.)
2 Instituto Pluridisciplina, Universidad Complutense de Madrid, Paseo Juan XXIII 1, Ciudad Universitaria, 28040 Madrid, Spain
3 Departamento de Física Aplicada, Universidad de Granada, Campus de Fuentenueva s/n, 18071 Granada, Spain; julia@ugr.es
* Correspondence: eduardogs@quim.ucm.es (E.G.); fortega@quim.ucm.es (F.O.);
Tel.: +34-913944107 (E.G.); +34-913944138 (F.O.)

**Abstract:** This study investigates the effect of an inert salt (NaCl) on the equilibrium interfacial tension and dilatational modulus of Pluronic F-68 copolymer, a triblock copolymer consisting of two terminal blocks of poly(ethylene oxide) and a less hydrophilic central block of poly(propylene oxide). Interfacial tension measurements were carried out using a surface force balance and a drop shape tensiometer, while rheological measurements were carried out in two different frequency ranges. This involved the use of the oscillatory barrier/droplet method and electrocapillary wave measurements, complemented by an appropriate theoretical framework. This work aimed to elucidate the influence of NaCl on the interfacial behavior of Gibbs monolayers of Pluronic F-68. In addition, this study highlights some of the technical and theoretical limitations associated with obtaining reliable dilatational rheological data at high frequencies (<1 kHz) using electrocapillary wave measurements. The results provide valuable insights into the interplay between salt presence and interfacial properties of Pluronic F-68 and highlight the challenges of obtaining accurate dilatational rheological data under specific measurement conditions.

**Keywords:** dilational rheology; electrocapillary waves; interfacial tension; ionic strength; copolymer; water/air interface

## 1. Introduction

Poly(ethylene oxide)$_n$–b–poly(propylene oxide)$_m$–b–poly(ethylene oxide)$_n$—or PEO–PPO–PEO—triblock copolymers, commonly referred to as Pluronics or Synperionics, are a family of polymeric materials that has gained a lot of attention in both scientific and manufacturing fields. These copolymers are known for their excellent biocompatibility and are used for making coatings, drug delivery devices, and thickeners, among many other applications. Their distinct structure, made up of ethylene oxide and propylene oxide blocks, allows for a wide range of functions, making them extremely valuable in numerous technological areas, including cosmetics, pharmaceuticals, food science, catalysis, and materials science [1–7]. The multifaceted utility of Pluronic copolymers derives from their distinctive surfactant properties, which enable them to modify surface interactions and stabilize different types of systems, including emulsion droplets, colloidal particles, capsules, or liposomes [8–11]. In addition, their remarkable versatility enhances material properties, including drug solubility, mechanical strength, and biodegradability in various matrices. One of the most fascinating features of Pluronics is their capacity to reduce

protein adsorption on solid surfaces. This has significant implications, notably in biomedical applications where avoiding undesired protein adsorption (biofouling) is critical for implantable devices, biosensors, and drug delivery systems [12,13].

To date, several studies have provided comprehensive insights into the intricate phase behavior of Pluronic solutions [14–17]. These studies have meticulously outlined the rich phase diagrams exhibited by these systems, revealing the existence of a wide range of phases including isotropic liquid, spherical, and rod-like micellar phases, as well as lamellar and gel phases [18–20]. It is worth noting that adding salt, which increases the ionic strength of the solution, does not impact the fundamental structure of the phase diagram. In fact, it remains qualitatively unaltered, providing a consistent framework under different conditions. However, the introduction of salts modifies the specific area occupied by each phase within the system [16,20–22]. For instance, the addition of ionic salts can reduce the solubility of Pluronic molecules in water and disrupt the micellar structure [23]. These modifications, intricately linked to the Hofmeister series but also to the specific ratio between the number of monomers in the poly(ethylene oxide) and poly(propylene oxide) blocks, establish a relationship between the behavior of ions as promoters or disruptors of water's structural stability, depending on their ability to remain hydrated [22,24,25]. Such intricate correlations between ionic properties and phase changes within Pluronic solutions continue to foster further investigations to unravel the underlying mechanisms governing these complex systems [23,24,26]. This has revealed that some ions can interact with the polymer chains in a very specific way, leading to behavior that cannot be explained by the Hofmeister series [27,28]. In fact, several studies have suggested that ions act only locally on the water structure [29–31].

Many of the applications of Pluronics involve complex mixtures containing salts, e.g., those in biological systems, in some cases at non-negligible concentrations, and rely on the ability of this type of copolymer to adsorb at fluid–fluid interfaces. Understanding the effect of salts on the interfacial behavior of Pluronic solutions is, therefore, essential to exploiting the full potential of this family of polymers [3,32,33]. However, to date, the effect of salt on the formation of Pluronic layers at the air/solution interface and the properties of such layers have been less explored, and only a few works can be found in the literature [34–36]. These works suggest that the effect of salts in Pluronic-laden interfaces responds to a complex interplay between the modification of the water structure at the copolymer/water interface and the adsorption of ions on the hydrophobic part of the copolymer. This has a dramatic effect on the interfacial properties with respect to salt-free solutions [36–38].

In a previous work [36], we have shown that the effect of $Li^+$ ions on the air/solution interface when Pluronic layers are present does not follow the Hofmeister series due to the specific interaction of lithium cations with the ether groups of PEO. In fact, the polydentate character of PEO allows the coordination of $Li^+$ ions through the oxygen [39,40]. This does not occur with other cations such as $Na^+$ and $K^+$, which have a direct interaction with the ether group of PEO blocks but no evidence of a true coordination is reported [41]. Therefore, the work by Llamas et al. [36] cannot be used to shed light on the effect of ionic strength alone. It is expected that the ionic strength will modify the solubility of Pluronics in the subphase, thus changing the formation of loops and tails in pure water at low frequencies [42]. This phenomenon was also observed in insoluble polystyrene–PEO–polystyrene monolayers [38].

This work aims to investigate the influence of an inert salt (NaCl) on the equilibrium interfacial tension and the dilatational modulus of Pluronic F-68 copolymer, a triblock copolymer with two lateral blocks of poly(ethylene oxide) formed by 76 monomers (3.35 kDa) and a central block of poly(propylene oxide) composed of 29 monomers (1.7 kDa). For this study, the combination of interfacial tension measurements and rheological measurements in two different frequency ranges obtained by combining the oscillatory barrier/droplet method and electrocapillary wave measurements with an appropriate theoretical background was applied. This allows one to elucidate the role of salt in the interfacial behavior of Pluronic F-68-laden interfaces as well as to point out some of the technical and theoretical

limitations in obtaining reliable dilational rheological data at high frequencies (in the range 50 Hz–1 kHz) using electrocapillary wave measurements.

## 2. Materials and Methods

### 2.1. Chemicals

Pluronic F-68, with an average molecular weight of 8.4 kDa, and NaCl with purity > 99.9% were supplied by Sigma-Aldrich (Saint Louis, MO, USA). Ultrapure deionized water of Milli-Q grade, with a resistivity higher than 18 MΩ·cm and a total organic content (TOC) of less than 6 ppm, was used for all experiments and material cleaning purposes. To achieve this level of purity, a Young Lin Instrument Co., Ltd. (Gyeonggi-do, Republic of Korea), AquaMAX™-Ultra 370 Series multi-cartridge purification system was used. All solutions were prepared by weight using an analytical balance accurate to ±0.01 mg. Throughout the experiments, temperature was maintained at 23.0 °C with an accuracy of ±0.1 °C.

### 2.2. Experimental Methods

2.2.1. Equilibrium Interfacial Tension Measurements

The interfacial tension of the air/solution interface was measured by using two different surface force tensiometers and a drop shape tensiometer. The measurements obtained with each tensiometer agreed within the combined error bar (approximately ±1 mN/m). For all the measurements, the temperature was controlled by using a thermostatic bath set at 23 °C. Each experimental data point reported was an average of at least three independent measurements. The experiments were conducted for a long enough time to ensure that a steady state was reached.

1.  Surface force tensiometer: A surface force tensiometer, specifically a K10T Digital Tensiometer (KRÜSS GmbH, Hamburg, Germany), fitted with a platinum Wilhelmy plate contact probe of 40.5 mm in perimeter. Between each measurement, the platinum plate was cleansed using ethanol and Milli-Q water and then burnt with an ethanol torch to eliminate any remaining residue of organic matter. For the measurements, the samples were poured into a glass cell, previously cleaned with ethanol and Milli-Q water.

    Additionally, we used a NIMA PS4 surface force tensiometer manufactured by Nima Technology (Coventry, UK) fitted with disposable Wilhelmy paper plates (Whatman CHR1 chromatography paper, Merck, Darmstadt) of 20.6 mm in perimeter. A fresh paper plate was used for each measurement to prevent any potential modifications to the plate surface caused by material adsorption. The same glass cells used for the measurements obtained using the KRÜSS K10T Digital Tensiometer (KRÜSS GmbH, Hamburg, Germany) were used in this case.

2.  Shape profile analysis tensiometer: The interfacial tension of the air/solution interface was also measured by a drop profile analysis tensiometer designed and fabricated at the University of Granada. This device was based on the Axisymmetric Drop Shape Analysis (ADSA) method, which is described in detail elsewhere [43]. The setup, including the image capturing, the microinjector, the ADSA algorithm, and the fuzzy pressure control, was managed by a Windows-integrated program (DINATEN(R)) [44]. For the experiments, a solution microdroplet (15 μL) was formed at the tip of a PTFE capillary (0.2 cm) introduced in a thermostatized glass cuvette (Hellma GmbH & Co. KG, Müllheim, Germany). This led to experiments characterized by a Worthington number, Wo, above 0.4, which guaranteed good precision of the experimental results [45].

2.2.2. Interfacial Dilational Rheology Measurements

Three different experimental techniques were used to study the dilational rheological response of the Gibbs monolayers of the Pluronic F-68 in two different frequency ($\nu$) ranges. In the low-frequency range ($10^{-3}$–$10^{-1}$ Hz), two different techniques were used:

(i) oscillating barrier measurements in a Langmuir balance (model 702 from Nima Technology, Coventry, UK) with a total area of 700 cm$^2$ (70 cm length $\times$ 10 cm width) and (ii) oscillating drop measurements, using a deformation amplitude of 8%, in the same drop profile analysis tensiometer used for equilibrium interfacial tension measurements. For obtaining data on the dilational response at higher frequencies (in the range of 10–10$^3$ Hz), a homemade electrocapillary wave device has been used [46,47]. In order to minimize the effect of shear on the results obtained using the oscillatory barrier method, the experiments were carried out using a relatively small deformation amplitude (5%). In addition, the paper Wilhelmy plate was placed parallel to the barrier movement in the center of the trough and the barrier oscillations were performed far enough from the contact probe to avoid any possible role of unintended flows in the dilation response.

The three techniques and the methods for calculating $\varepsilon_r$ from the raw data have already been described in detail previously [48,49]. It should be noted that the imaginary component of the dynamic interfacial elasticity ($\varepsilon_i$) related to the viscous loss (loss modulus) remained below 5% of the real component or storage modulus ($\varepsilon_r$) in all measurements. As a result, the detailed discussion of the imaginary part provides limited insight into the clarity of the work and is, therefore, not discussed here. It is worth noting that the low values obtained for the loss modulus in this study agree with previous results for adsorption layers formed by different copolymers of the Pluronic family at fluid interfaces [37,50].

### 2.2.3. Bulk Viscosity Measurements

A capillary-based method (Ubbelohde viscometer) was used to measure the bulk viscosity of the samples. The liquid was introduced into a glass viscometer thermostatized at 23 °C and pumped up through a capillary and a measuring bulb and the time taken for the liquid to fall through the bulb was recorded. The viscometer was calibrated against filtered Milli-Q water and each sample was filtered before entering the viscometer. The determination of viscosity is based on the assumption that the flow time is directly proportional to the viscosity and inversely proportional to the density of the solution.

## 3. Results and Discussion

### 3.1. Interfacial Tension Isotherm

Figure 1 shows the interfacial tension ($\gamma$) isotherm for the Gibbs monolayers obtained by the adsorption of aqueous solutions of Pluronic F-68 (ionic strength: 0 mM) at 23 °C to the air/solution interface. The results show that after the initial sharp decrease in interfacial tension with Pluronic F-68 concentration ($c$), from values close to those corresponding to the pristine air/solution interface, the interfacial tension isotherm enters a less steep reduction region, commonly defined as a pseudo-plateau, for concentrations in the range 10$^{-4}$–10$^{-2}$ mM; this can be seen more clearly in the surface pressure representation (see inset of Figure 1). The existence of such a pseudo-plateau has been observed in previous studies on the adsorption properties of Pluronic F-68 at the air/solution interface, and it is commonly ascribed to the transition from a dilute interfacial layer to a brush organization of the Pluronic F-68 at the interface [36,48,51]. Once the pseudo-plateau region is overcome, the interfacial tension starts to decrease again with the Pluronic F-68 concentration. It is worth noting that in the present study, the investigated concentration range remains below the critical micelle concentration (CMC) of Pluronic F-68 (around 10 mM) [52,53] in agreement with the continuous decrease in interfacial tension recorded. It should be noted that for the investigated region, the interfacial tension values obtained are in agreement with the interfacial tension isotherms reported in the literature for the same copolymer under similar conditions [36,54].
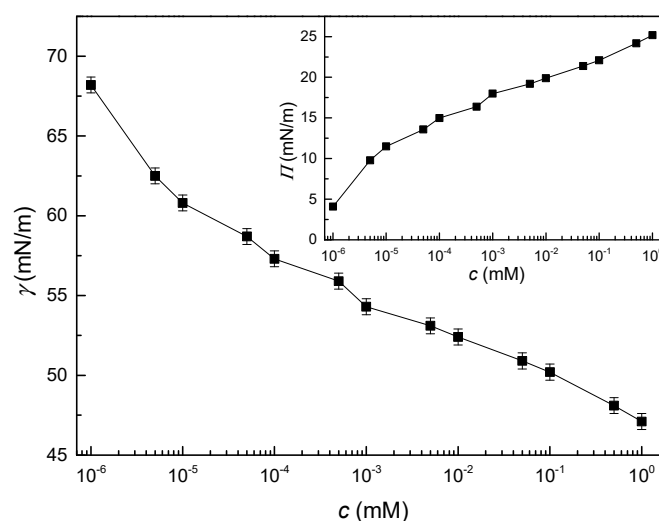
**Figure 1.** Interfacial tension as a function of concentration (*c*), at 23 °C, for Gibbs monolayers of Pluronic F-68 at the air/solution interface. Inset corresponds to interfacial pressure ($\Pi = \gamma_0 - \gamma$), where $\gamma_0$ is the pure water surface tension at the same temperature. The line is a guide for the eyes.

Figure 2 shows a sketch of the different configurations of Pluronic F-68 at the air/solution interface as a function of interfacial density. At high interfacial tensions, corresponding to high surface pressures and low surface excesses, the chains are placed at the interface forming a layer of 2D stretched chains. Then, for intermediate interfacial tensions, corresponding to the pseudo-plateau of the isotherm, the copolymer molecules start to reorganize at the interface and undergo stretching into the aqueous phase. Finally, at the lowest values of surface tension, most of the copolymer molecules adopt a brush organization to form a 3D structure [50].
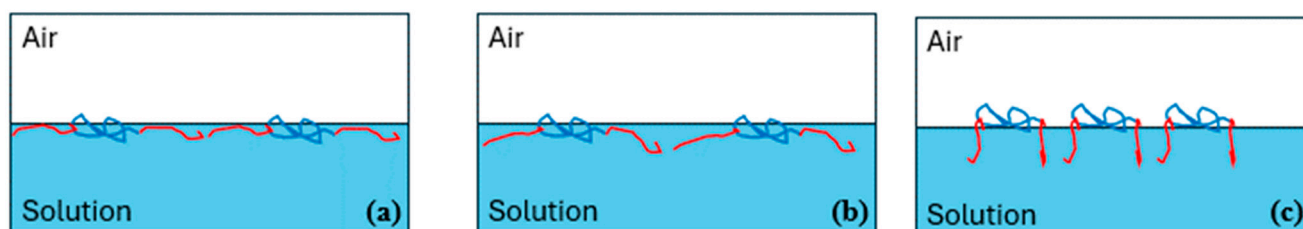


**Figure 2.** Sketch of the different conformations of Pluronic F-68 at the air/solution interface. (**a**) High interfacial tension values. (**b**) Intermediate interfacial tension values (pseudo-plateau region). (**c**) Low interfacial tension values. The central poly(propylene oxide) blocks are indicated in blue and the lateral poly(ethylene oxide) blocks are represented in red.

Considering that the main aim of this work is to elucidate how the change in the ionic strength (*I*) of the solution by the addition of NaCl affects the equilibrium properties and dilational rheological response of Gibbs monolayers of Pluronic F-68, interfacial tension measurements were performed for solutions with different copolymer concentrations by varying *I*. Figure 3 shows the dependence of the interfacial tension on the ionic strength of the solution for the adsorption of Pluronic F-68 with different copolymer concentrations at the aqueous air/solution interface. The results show that an increase in ionic strength produces a very marked decrease in surface tension, compared to the Gibbs monolayers in the absence of salt. This is exactly the opposite behavior to that expected for the change in interfacial tension at the air/water interface due to salt addition (see Appendix A). However, this is not an unexpected result, as previous studies with different copolymers belonging to the Pluronic family have shown that the addition of electrolytes to Pluronic solutions induces a salting-out phenomenon, which enhances the surface activity of the copolymer and, thus, leads to a strong decrease in the interfacial tension [16,36]. This can be understood by the fact that the electrolytes disrupt favorable PEO–water interaction,

leading to a dehydration of the hydrophilic blocks, which in turn results in an increase in the hydrophobicity of the copolymer and enhances their adsorption efficiency to the air/solution interface.
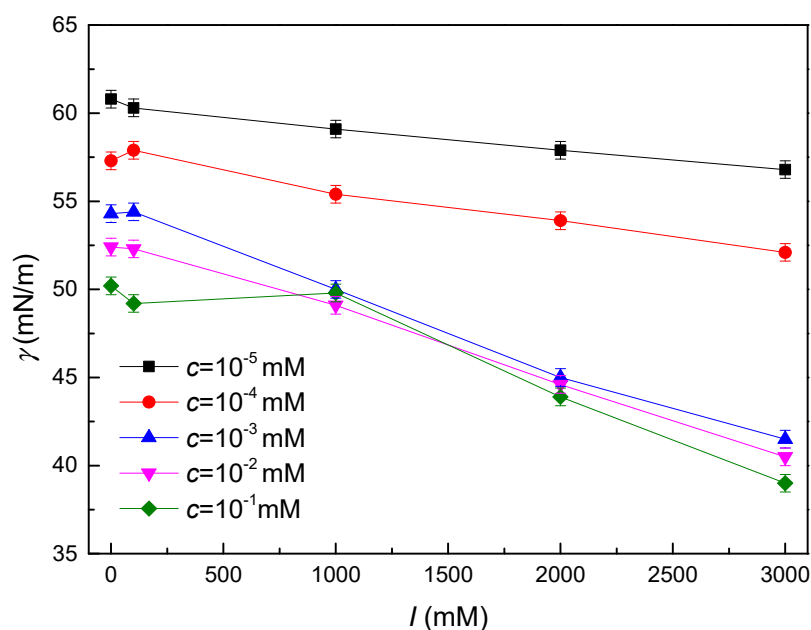


**Figure 3.** Ionic strength ($I$) dependence of the interfacial tension ($\gamma$) at 23 °C for the adsorption of Pluronic F-68 solutions of different concentrations at the air/solution interface. The symbols correspond to the experimental data, and the lines are guides for the eyes.

A detailed analysis of the dependence of the interfacial tension on the ionic strength evidences that the salting-out produced by NaCl addition is almost negligible for low salt concentrations, independent of the copolymer concentration. However, when $I$ reached values $\geq 1$ M, the presence of the electrolyte leads to a significant enhancement of the surface activity of Pluronic F-68, corresponding to an increase in copolymer surface excess, and the higher the copolymer concentration, the greater the effect. It is worth noting that the observed effect of ionic strength is only evidenced for NaCl concentrations above those typically studied in most of the work in the literature.

### 3.2. Low-Frequency Dilational Rheology

The first step in the evaluation of the interfacial response against dilational deformations was carried out at low frequencies (in the range of $10^{-3}$–$10^{-1}$ Hz). For this purpose, oscillatory barrier and oscillatory droplet experiments were performed. The results obtained by both techniques show good agreement within the combined error bars (see Figure 4a). Figure 4b,c shows the frequency dependences of the dilational storage modulus obtained for Gibbs monolayers of Pluronic F-68 at different ionic strengths.

The obtained results evidence, independently of the Pluronic F-68 concentration and the ionic strength, a similar qualitative behavior characterized by the increase in the dilational storage modulus with the deformation frequency. This frequency dependence suggests the existence of a relaxation process for a frequency around $10^{-2}$–$10^{-1}$ Hz which agrees with previous results by Rivillon et al. [38] for Gibbs monolayers of Pluronic copolymers. The emergence of this relaxation process can be ascribed to the diffusion process of the Pluronic F-68 from the bulk to the interface.
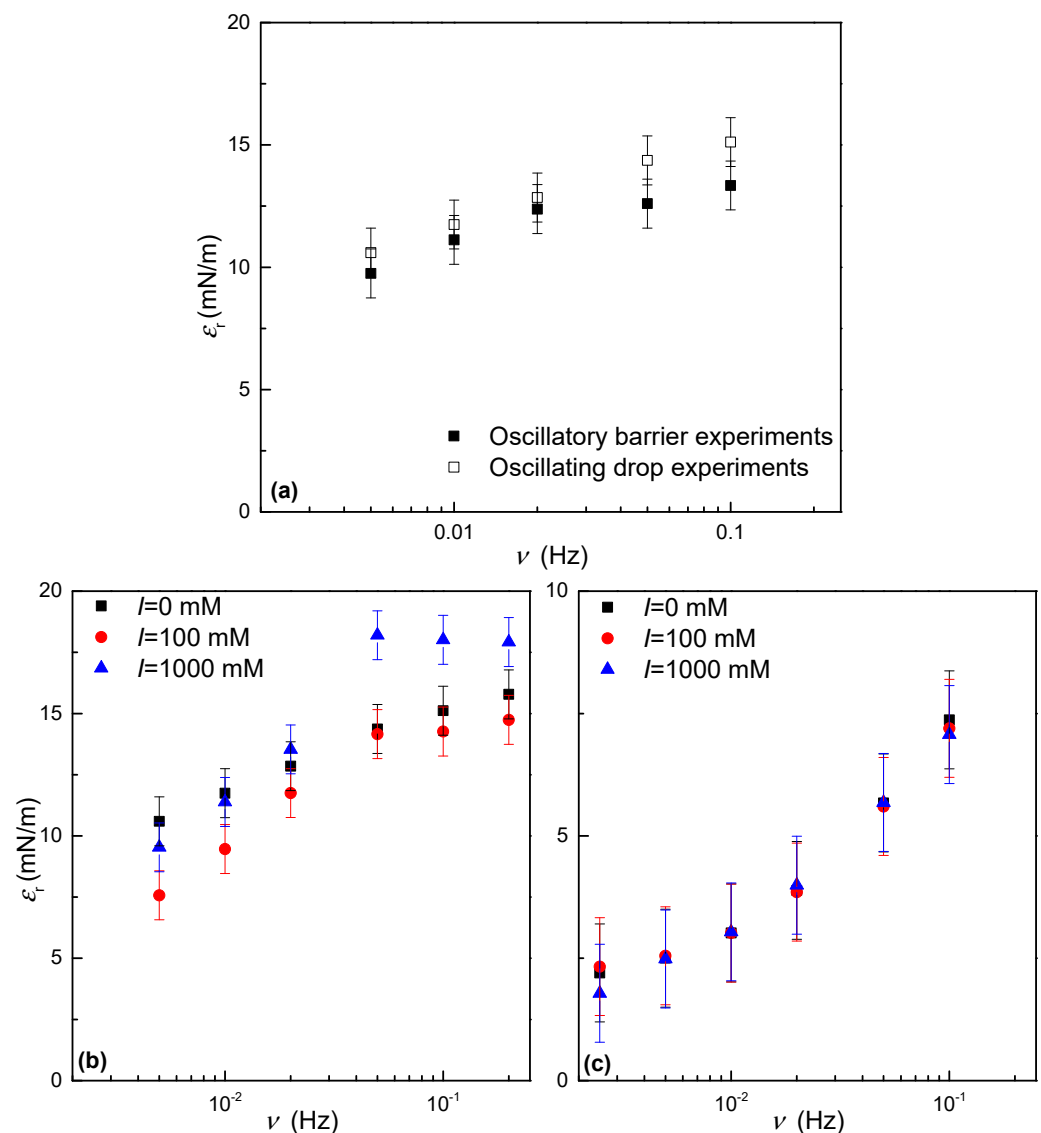
**Figure 4.** (**a**) Frequency dependence of the storage modulus ($\varepsilon_r$) obtained by oscillatory barriers and oscillating drop measurements at 23 °C for Gibbs monolayers obtained for the adsorption of Pluronic F-68 solutions of concentration $10^{-3}$ mM and a fixed ionic strength of 0 mM. (**b**) Frequency dependence of the storage modulus ($\varepsilon_r$) at 23 °C for Gibbs monolayers obtained for the adsorption of Pluronic F-68 solutions of $c = 10^{-3}$ mM and different ionic strengths at the air/solution interface. (**c**) Frequency dependence of the storage modulus ($\varepsilon_r$) at 23 °C for Gibbs monolayers obtained for the adsorption of Pluronic F-68 solutions of $c = 10^{-1}$ mM (**b**) and different ionic strengths at the air/solution interface.

Further considering the dilational storage modulus dependences on the concentration of Pluronic F-68 and ionic strength, it can be observed that the variation in the ionic strength within the range 0-1 M does not present any strong impact on the values of the dilational modulus at low frequencies, even though for an ionic strength of 1 M and polymer concentration of $10^{-3}$ mM, a slight increase in the storage modulus is observed. However, this does not occur for the Gibbs monolayers obtained by the adsorption of solutions of higher concentration ($10^{-1}$ mM) where the dilational storage modulus remains unchanged by increasing the ionic strength of the aqueous phase. This is clearer from Figure 5a where the dependence of the storage modulus on the ionic strength at a fixed frequency of $5 \times 10^{-2}$ Hz is displayed. The explanation for this different effect of the salt depending on the copolymer concentration can be understood from the data shown

in Figure 3. Indeed, for the lowest concentration of Pluronic F-68 ($10^{-3}$ mM), a strong change in interfacial tension is observed with the ionic strength, whereas for solutions with a concentration of $10^{-1}$ mM, the change is almost negligible. This suggests a salt-induced conformational change in the former case, which increases the value of the dilatational storage modulus. This is in agreement with previous studies on the influence of ionic strength on the rheological properties of polymer-loaded interfaces [55].
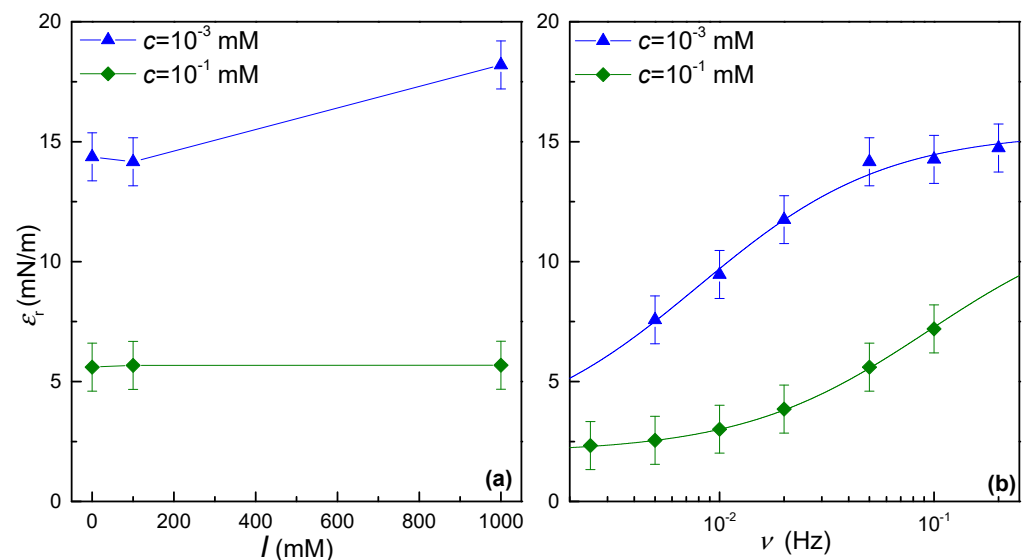


**Figure 5.** (**a**) Dependence of the storage modulus at a fixed frequency of $5 \times 10^{-2}$ Hz on the ionic strength for Gibbs monolayers of Pluronic F-68 at two different bulk concentrations. The symbols correspond to the experimental data, and the lines are guides for the eyes. (**b**) Frequency dependence of the storage modulus ($\varepsilon_r$) for Gibbs monolayers obtained for the adsorption of Pluronic F-68 solutions of two different concentrations, $c = 10^{-3}$ mM and $c = 10^{-1}$, and at a fixed ionic strength (100 mM). The symbols correspond to the experimental data, and the lines corresponds to the best fit obtained using the Lucassen–van den Tempel model.

The Pluronic F-68 concentration also affects the relaxation spectrum in the considered frequency range. This is better understood with Figure 5b where the frequency dependence of the dilational storage modulus at a fixed ionic strength of 100 mM is reported for the two concentrations of Pluronic F-68. The results evidence that the increase in the Pluronic F-68 concentration from $10^{-3}$ mM to $10^{-1}$ mM shifts the relaxation process found within the considered frequency range to higher values of the characteristic frequency. This is clearer from the analysis of the experimental data in terms of the Lucassen–van den Tempel model given by the following equation [56]:

$$\varepsilon(\nu) = \varepsilon_0 \frac{1 + \zeta + i\zeta}{1 + 2\zeta + 2\zeta^2}, \tag{1}$$

where $\varepsilon(\nu) = \varepsilon_r(\nu) + i\varepsilon_i(\nu) = \varepsilon_r(\nu) + i2\pi\nu\kappa$ is the interfacial dilational viscoelastic modulus, with $\kappa$ defining the interfacial dilational viscosity, and $\varepsilon_0$ is the Gibbs elasticity, and $\zeta = \nu_D/\nu$ is a parameter defining the exchange of matter between the interface and the adjacent bulk phase, with $\nu_D$ being the characteristic frequency of the relaxation process. Figure 6 reports the best-fit parameters obtained from the analysis in terms of the Lucassen–van den Tempel model for the studied Gibbs monolayers.
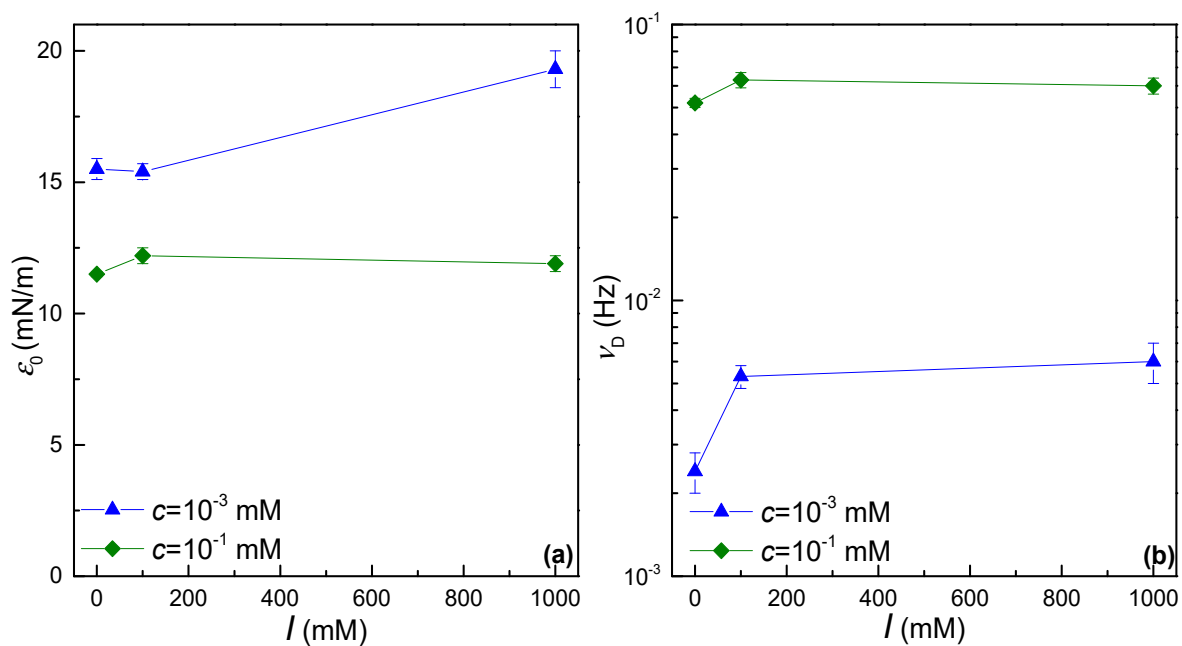
**Figure 6.** Dependence of the best fit parameters obtained using the Lucassen–van den Tempel model, $\varepsilon_0$ (**a**) and $\nu_D$ (**b**), on the ionic strength for Gibbs monolayers of Pluronic F-68 at two different bulk concentrations. The symbols correspond to the experimental data, and the lines are guides for the eyes.

The dependence of $\varepsilon_0$ on the ionic strength of the Pluronic F-68 solutions agrees with the above dependence of the values of $\varepsilon_r$. On the other hand, the dependences of the characteristic frequencies of the relaxation process on the ionic strength appear more interesting (see Figure 6b). Firstly, the results confirm the above-discussed scenario related to the increase in the value of the characteristic frequency as the copolymer concentration increases from $10^{-3}$ mM to $10^{-1}$ mM. In fact, the results evidence an increase of about one order of magnitude for the characteristic relaxation frequency. This indicated that the exchange process between the bulk and the interface occurs with a higher probability at higher concentrations, which is the expected result. In addition, independent of the copolymer concentration, the increase in the ionic strength leads to an increase in the characteristic relaxation frequency. This can be explained by considering the worsening of the solvent quality of the subphase for Pluronic F-68 with the increase in the ionic strength. This is expected to favor the surface adsorption of the copolymer molecules and a corresponding decrease in the characteristic diffusion time.

### 3.3. High-Frequency Dilational Rheology: Electrocapillary Wave Damping Measurements

The evaluation of the damping of capillary waves excited by electric fields as a result of the presence of Pluronic F-68 Gibbs monolayers at the air/solution interface allows one to obtain information on the dilational interfacial rheological response at higher frequencies (above 50 Hz) than typical oscillatory rheology. Therefore, the combination of electrocapillary wave damping measurements with the above-discussed results contribute to expanding the accessible frequency region of the dilation spectrum. It should be noted that electrocapillary wave experiments were performed in the frequency range of 80–400 Hz. It was not possible to perform experiments over 400 Hz due to the strong decrease in the intensity of the signal that significantly reduced the sensibility of the measurements.

3.3.1. Study of Propagation of Capillary Waves as Pluronic F-68-Laden Interfaces

For a capillary wave excited in a point of the interface (*xy* plane) defined by the coordinate *x* = 0, it is possible to define its spatial profile in terms of damped cosine according to the following expression:

$$u_z = u_z^0 e^{-\beta x} \cos\left(\frac{2\pi}{\lambda} x + \varphi\right), \tag{2}$$

with $u_z^0$ being the wave amplitude and $\beta$, $\lambda$, and $\varphi$ the damping coefficient, the characteristic capillary wavelength, and the phase lag, respectively. Figure 7 shows the frequency dependence of the parameters $\beta$ and $\lambda$ for the two studied Pluronic F-68 concentration and different ionic strengths.
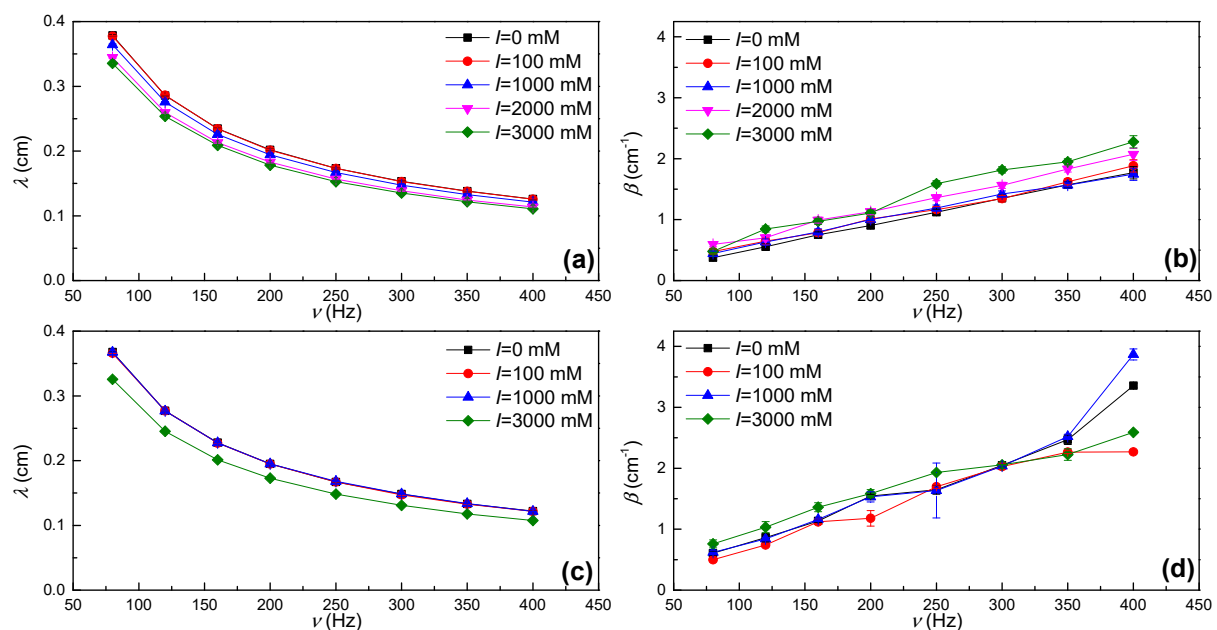


**Figure 7.** Frequency dependences of the wavelength ($\lambda$) and damping ($\beta$) for monolayers obtained from the adsorption of solutions of two different Pluronic F-68 concentrations at different ionic strengths. (**a**,**b**) $\lambda$ and $\beta$ values, respectively, for Pluronic F-68 solutions with a concentration of $10^{-3}$ mM and (**c**,**d**) $\lambda$ and $\beta$ values, respectively, for Pluronic F-68 solutions with a concentration of $10^{-1}$ mM. The lines are guides for the eyes.

The results show that at a fixed frequency, the capillary wavelength, $\lambda$, slightly decreases as the ionic strength increases, independently of the Pluronic bulk concentration. This is particularly evident when the NaCl concentration overcomes the threshold value of 1 M. These results can be rationalized by considering Kelvin's law ($\lambda^3 = 2\pi\gamma/\nu\rho$, where $\rho$ accounts for the bulk density) [57], although it must be taken into account that this equation is only valid for low-viscosity simple liquids. The decrease in $\lambda$ becomes stronger in the region where the variation in $\gamma$ with the ionic strength is higher (above NaCl concentration around 1M). On the other hand, Gibbs monolayers obtained from solutions of Pluronic F-68 concentration = $10^{-1}$ mM exhibit lower values of $\lambda$ than when the copolymer concentration is $10^{-3}$ mM. This may be also rationalized considering the reduction in the interfacial tension with the increase in Pluronic F-68 concentration (see Figure 3).

Interpretations of the dependencies of the damping coefficient are less straightforward (see Figure 7b,d). As occurred for the capillary wavelength, the effect of salt in the damping coefficient is almost negligible when ionic strength is below 1 M, whereas an increase in the ionic strength above such a threshold slightly increases the damping coefficient values. This can be rationalized as a combination of two different factors. First, the increase in the ionic strength results in an increase in the bulk viscosity of the solution (see Appendix A),

which according to the Stokes' law must lead to an increase in the damping coefficient [57]. The second factor that influences the increase in $\beta$ is the increase in the surface excess as a result of the salting-out phenomenon. It should be noted that the increase in the damping coefficient with the concentration of Pluronic F-68 should be ascribed to the higher amount of surfactant adsorbed at the interface, because the viscosity of Pluronic F-68 solutions does not significantly change within the studied concentration range.

A more detailed analysis of the frequency dependences of the capillary wavelength and damping coefficient shows that the experimental data can be described in terms of simple scaling laws $\omega \sim q^a$ and $\beta \sim \omega^b$, where $\omega = 2\pi\nu$ defines the angular frequency and $q = 2\pi/\lambda$ is the wavevector. In this study, the value obtained for the exponent $a$ is around 1.46 for all the studied conditions, which is similar to that predicted from Kelvin's law: $\omega \sim q^{3/2}$. On the contrary, the value of the exponent for the scaling law describing the frequency dependence of $\beta$ differs from the one that can be derived from Stokes' law ($b = 1$), and the differences increase with the ionic strength [57]. This suggests the possible existence of viscoelastic loss in the monolayer in agreement with previous studies on Pluronic monolayers in the absence of salt [54]. It should be noted that for the highest frequencies evaluated for Gibbs monolayers obtained from solutions with copolymer concentration of $10^{-1}$ mM, the damping coefficient values diverge from the general tendency which can be ascribed to a worsening of the signal quality.

To obtain information about the dilational response of the monolayer from electrocapillary wave experiments, we need to numerically solve the dispersion equation, $D(q, \omega) = 0$, which provides a relation between the characteristic parameters associated with the propagation of the transversal waves (frequency $\omega$, wavelength $\lambda$, and damping coefficient $\beta$) and the constitutive parameters of the monolayer (interfacial tension $\gamma$, dilational storage modulus $\varepsilon_r$, and dilational viscosity $\kappa$) [58,59].

$$D(q, \omega) = T(q, \omega, \gamma)L(q, \omega, \varepsilon) + C(q, \omega) = 0. \tag{3}$$

This indicates that the dilational rheological response of monolayers at the air/water interface is described by the coupling between the transversal or capillary $T(q, \omega, \gamma)$ and the longitudinal or dilational $L(q, \omega, \varepsilon)$ terms of the dispersion equation [60]. The solution of the dispersion equation provides a dilational modulus that is defined as

$$\varepsilon(\omega) = \varepsilon_r(\omega) + \varepsilon_i(\omega) = \frac{\frac{-(\eta\omega(q - m))^2}{\gamma q^2 + i\eta\omega(q + m) - \frac{\rho}{q}\omega^2} - i\eta\omega(q + m)}{q^2}, \tag{4}$$

where $q$ is the complex wavevector, defined as

$$q = \frac{2\pi}{\lambda} - i\beta, \tag{5}$$

and $m$ is the capillary penetration depth ($\text{Re}(m) > 0$)

$$m = \sqrt{q^2 + i\omega\frac{\rho}{\eta}}. \tag{6}$$

### 3.3.2. Accuracy of the Characterization of the Dilational Rheology by Electrocapillary Wave Measurements: The Resonance Condition

The extraction of the constitutive parameters of the monolayers from electrocapillary wave measurements is always challenging. This is mainly related to the change in the sensibility of capillary waves as response to the dilational properties of the interface. The resonance condition indicates that the frequency of the dilational modes is very close to that corresponding to the capillary ones, providing the highest sensibility of capillary waves for

the determination of $\varepsilon_r$ and $\kappa$ values. At a first approximation, the resonance occurs for the following interval:

$$\left(\frac{\varepsilon}{\gamma}\right)_R = \left(\frac{q\eta^2}{\gamma\rho}\right)^{1/4} \approx 0.10 - 0.15, \tag{7}$$

where the subindex R indicates the resonance condition. The resonance condition is of paramount importance for the determination of the dilational parameters from electrocapillary wave experiments. In fact, as the $\frac{\varepsilon}{\gamma}$ ratio differs from the resonance condition, the dilational parameters extracted from the analysis of the experimental data are affected by a high uncertainty. Figure 8 shows the $\varepsilon/\gamma$ ratio for all the analyzed samples.
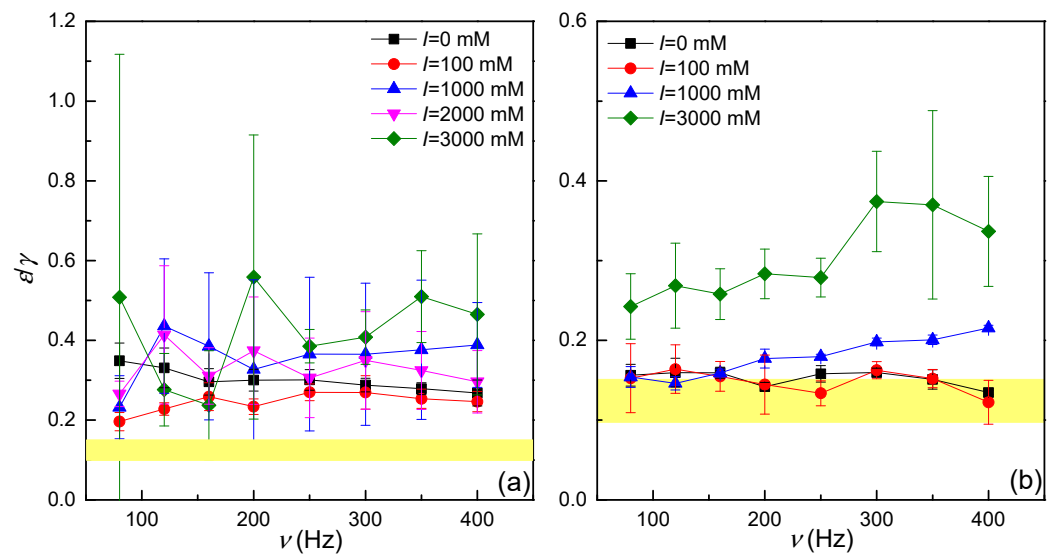


**Figure 8.** Frequency dependences of the $\frac{\varepsilon}{\gamma}$ ratio for monolayers obtained from solutions of two different Pluronic F-68 concentrations at different ionic strengths. (**a**) Pluronic F-68 solutions with a concentration of $10^{-3}$ mM and (**b**) Pluronic F-68 solutions with a concentration of $10^{-1}$ mM. The highlighted region corresponds to the expected resonance region, and the lines are guides for the eyes.

The results show that for the most diluted solution (concentration = $10^{-3}$ mM), the $\varepsilon/\gamma$ ratio differs significantly for the resonance condition. This indicates that small variations in the input parameters $\gamma$ and $\eta$ introduce a high uncertainty in the determination of $\varepsilon_r$ and $\kappa$. The situation is better, or at least when the values of the ionic strength are lowest, when the concentration of Pluronic F-68 is increased up to $10^{-1}$ mM. In this case, the values of the $\varepsilon/\gamma$ ratio are closer to the resonance condition. In particular, for an ionic strength below 1M, the $\varepsilon/\gamma$ ratio enters the resonance region. Therefore, the determination of the viscoelastic modulus is less affected by slight changes in $\gamma$ and $\eta$. Further considering the variation in the $\varepsilon/\gamma$ ratio with the ionic strength, it is clear that an increase in the ionic strength takes the monolayer behavior, independent of the copolymer concentration, far from the resonance condition. This is reflected in the value of the $\varepsilon/\gamma$ ratio but also in the increase in the uncertainty of this ratio. Therefore, the results point out that both bulk concentration and surface excess present a critical impact in the applicability of electrocapillary waves in the determination of the dilational properties of monolayers at the air/water interface in agreement with previous results by Maestro et al. [47].

Further considering the effect of the ionic strength on the value of the $\varepsilon/\gamma$ ratio, it is clear that the salting-out phenomenon, leading to an increase in the surface excess, increases the uncertainty of electrocapillary wave measurements for an accurate determination of the dilational behavior of Pluronic F-68 Gibbs monolayers. In fact, the higher the ionic strength, the higher the value of the $\varepsilon/\gamma$ ratio and the greater the distance from the resonance condition. In addition, the uncertainty in the determination of the true value of the $\varepsilon/\gamma$ ratio also increases

as evidenced by the increase in the error bars. However, the increase in the surface excess alone cannot be considered as the only effect worsening the quality of the determination of the dilational properties of the interface by electrocapillary wave measurements as evidenced the better quality of the results obtained for the highest studied concentration ($10^{-1}$ mM).

### 3.3.3. Dilational Spectrum: Combination of Oscillatory Rheology and Electrocapillary Wave Measurements

The combination of rheological experiments allowing one to assess the dilational properties of interfaces in different frequency ranges is a very powerful tool for obtaining information of whole mechanical relaxation spectrum for molecules attached to fluid/fluid interfaces [46,47]. Figure 9 displays the dependence of the storage modulus $\varepsilon_r$ on the frequency for Gibbs monolayers obtained by adsorption of solutions with two different concentrations of copolymer and different ionic strengths.
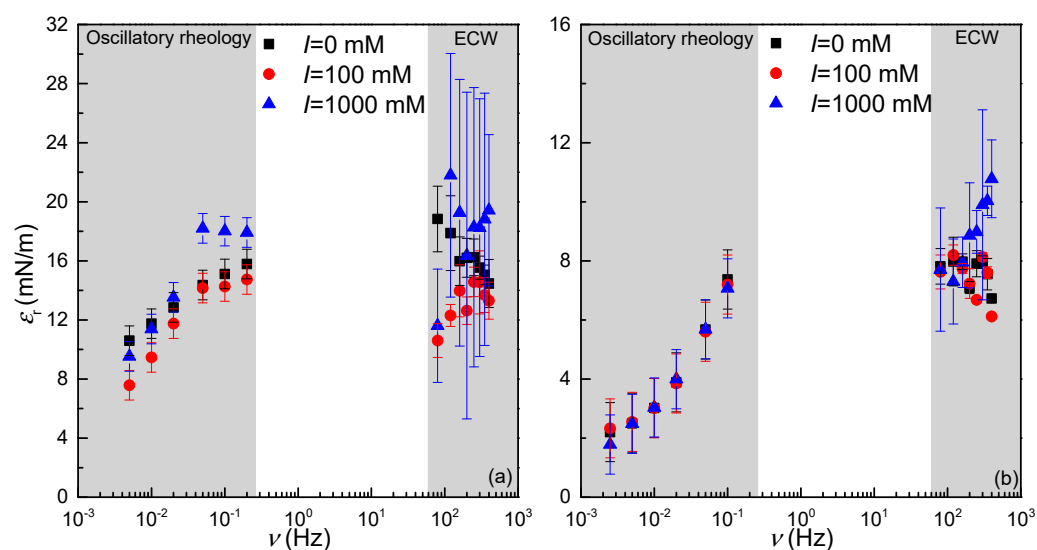


**Figure 9.** Frequency dependence of the storage modulus ($\varepsilon_r$) at 23 °C for Gibbs monolayers obtained for the adsorption of Pluronic F-68 solutions of two different concentrations, $c = 10^{-3}$ mM (**a**) and $c = 10^{-1}$ mM (**b**), and different ionic strengths at the air/solution interface. In the panels, the data correspond to oscillatory rheology and electrocapillary wave (ECW) experiments. The grey region indicates the different regions of accessible frequencies with the used devices.

The relaxation spectrum obtained by combining oscillatory dilational rheology and electrocapillary wave experiments is in good qualitative agreement with the results obtained only by using the measurements at a low frequency, with the storage modulus reducing its value across the whole frequency range as the Pluronic F-127 concentration increases from $10^{-3}$ mM up to $10^{-1}$ mM. Deepening on the analysis of the experimental results, it is confirmed that the storage modulus results obtained for conditions far from the resonance situation are affected by higher uncertainty. This is clear from the huge errors bars associated with the results obtained for Gibbs monolayers corresponding to a bulk concentration of $10^{-3}$ mM. On the contrary, the error bars are less important for experiments obtained from the adsorption of Pluronic F-68 solutions with concentration = $10^{-1}$ mM, where the $\varepsilon/\gamma$ ratio is closer to that corresponding to the resonance. This is clearer for the storage results obtained for an ionic strength below 1000 mM, where an overlapping of the $\varepsilon/\gamma$ ratio with the resonance region was found. However, the increase in the ionic strength worsens the accuracy of the determination of the storage modulus as evidenced by the bigger error bar. However, the latter remains below the uncertainty of the determination of the storage modulus for Gibbs monolayers obtained from Pluronic F-68 solutions of concentration = $10^{-3}$ mM. The above discussion is clearer from the results in Figure 10 where the values of the storage modulus obtained from electrocapillary wave experiments in the frequency range of 80–400 Hz are

depicted for Gibbs monolayers obtained at two different bulk copolymer concentrations and different ionic strengths. The results evidence that in the case of Gibbs monolayers obtained from solutions with concentration = $10^{-3}$ mM, the uncertainty associated with the determination of storage modulus values is huge, making it difficult to obtain any dependence of the storage modulus on the ionic strength on the subphase. On the other hand, the results obtained by electrocapillary wave experiments do not evidence any dependence of the storage modulus on the frequency for the Gibbs monolayer obtained from solutions at concentration of $10^{-3}$ mM. The situation changes when the copolymer concentration is increased. In this case, the values of the storage modulus tend to increase with the ionic strength of the solution in agreement with the results reported by Llamas et al. [36] in systems containing lithium salts. In addition, the increase in the ionic strength above 1 M introduces a frequency dependence on the storage modulus, which indicates the existence of a relaxation mechanism with a characteristic frequency in the range of $10^2$–$10^3$ which can be ascribed to the reorganization of the copolymer molecules within the interface.
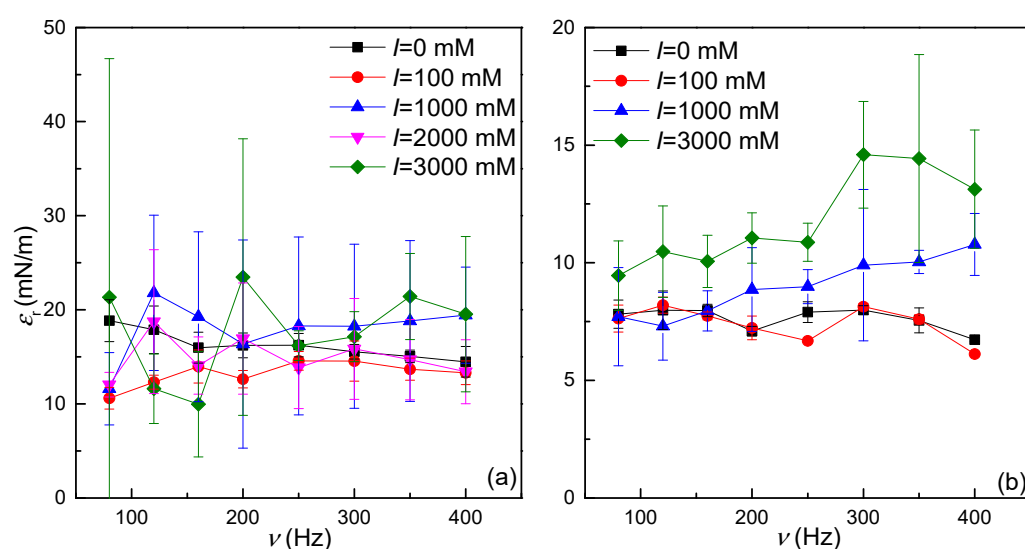


**Figure 10.** Frequency dependence of the storage modulus ($\varepsilon_r$) at 23 °C for Gibbs monolayers obtained by electrocapillary wave experiments for the adsorption of Pluronic F-68 solutions of two different concentrations, $c = 10^{-3}$ mM (**a**) and $c = 10^{-1}$ mM (**b**), and different ionic strengths at the air/solution interface. The lines are guides for the eyes.

Based on the above results, it is clear that the best theoretical representation of the dilational response of Pluronic F-68 Gibbs monolayers at the lowest concentration of copolymer studied in this work ($10^{-3}$ mM) is the Lucassen–van den Tempel model (see Equation (1)). This also provides a good representation for the dilation relaxation spectrum of Gibbs monolayers obtained from solutions with concentration = $10^{-1}$ mM, at least at the lowest ionic strengths. However, when the ionic strength reaches a value of 1 M, a second contribution must be included to describe the dilational spectrum [36,46,60]. For this purpose, we followed the procedure introduced by Ravera et al. [46,60] which provides a description for an interfacial relaxation spectrum characterized by the presence of diffusion-controlled adsorption and interfacial relaxation according to the following expression:

$$\varepsilon = \frac{1 + \zeta + i\zeta}{1 + 2\zeta + 2\zeta^2}\left(\varepsilon_0 + (\varepsilon_1 - \varepsilon_0)\frac{1 + i\chi}{1 + \chi^2}\right), \tag{8}$$

where $\varepsilon_1$ is the high-frequency limit of the dilational elasticity and $\chi = \nu_1/\nu$ a parameter describing the interfacial relaxation process, with $\nu_1$ being the characteristic frequency of the interfacial relaxation process. Figure 11 shows the best fits obtained for the dilational spectrum of Gibbs monolayers obtained from the adsorption of Pluronic F-68 solutions with different concentration and a fixed ionic strength.
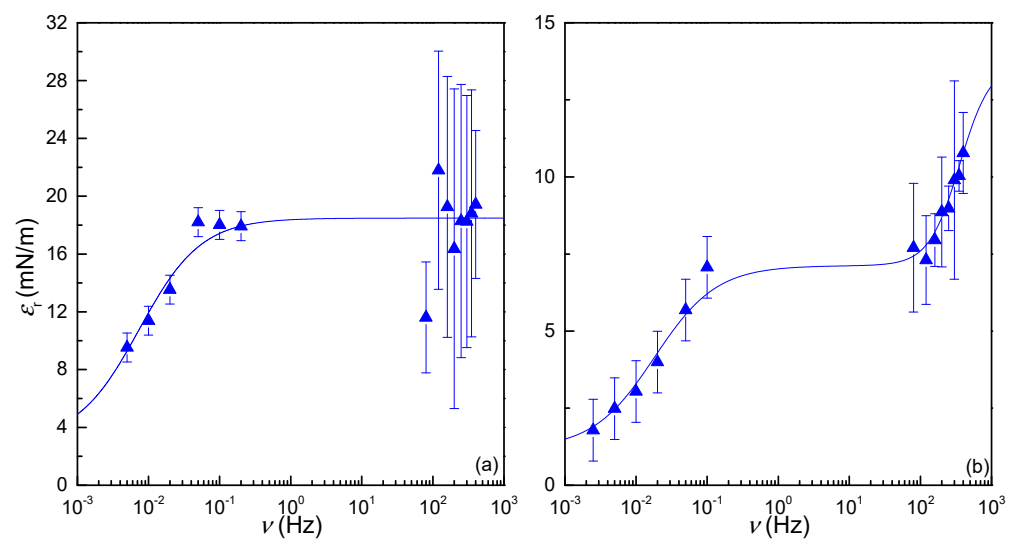
**Figure 11.** Frequency dependence of the storage modulus ($\varepsilon_r$) at 23 °C for Gibbs monolayers obtained for the adsorption of Pluronic F-68 solutions of two different concentrations, $c = 10^{-3}$ mM (**a**) and $c = 10^{-1}$ mM (**b**), and a fixed ionic strength of 1000 mM. In the panels, the symbols correspond to the experimental data obtained by oscillatory rheology and electrocapillary wave (ECW) experiments, and the lines are the best fit to the theoretical model described by Equations (1) and (8).

The above results evidence that the Lucassen–van den Tempel model or its combination with an additional relaxation process provides a suitable description of the dilational spectrum of Gibbs monolayers of Pluronic F-68. Table 1 reports the limit elasticities, $\varepsilon_0$ and $\varepsilon_1$, and the characteristic frequencies of the relaxation processes, $\nu_D$ and $\nu_1$, obtained from the fitting of the experimental data across the whole frequency range to the Lucassen–van den Tempel model or to its extension by including an additional process occurring within the interface. Notice that the Lucassen–van den Tempel model accounts for the rheological response of Gibbs monolayers obtained from Pluronic solutions with concentration = $10^{-3}$ mM, independent of the ionic strength, whereas in the case of monolayers obtained from the adsorption of solutions with concentration = $10^{-1}$ mM, one needs to use an extension of the Lucassen–van den Tempel model including the additional interfacial process.

**Table 1.** Summary of the limit elasticities, $\varepsilon_0$ and $\varepsilon_1$, and the characteristic frequencies of the relaxation processes, $\nu_D$ and $\nu_1$, obtained from the fitting of the experimental data across the whole frequency range to the Lucassen–van den Tempel model or to its extension by including an additional process occurring within the interface.

| $c$ (mM) | $10^{-3}$ | | $10^{-1}$ | | | |
|---|---|---|---|---|---|---|
| $I$ (mM) | $\varepsilon_0$ (mN/m) | $10^3 \nu_D$ (Hz) | $\varepsilon_0$ (mN/m) | $10^2 \nu_D$ (Hz) | $\varepsilon_1$ (mN/m) | $10^{-2}\nu_1$ (Hz) |
| 0 | 15.6 ± 0.2 | 2.5 ± 0.4 | 7.7 ± 0.1 | 1.5 ± 0.2 | - | - |
| 100 | 14.1 ± 0.2 | 3.7 ± 0.8 | 7.4 ± 0.2 | 1.3 ± 0.3 | - | - |
| 1000 | 18.5 ± 0.4 | 6 ± 1 | 7.1 ± 0.3 | 1.2 ± 0.3 | 14 ± 1 | 3.6 ± 0.7 |

## 4. Conclusions

This work evaluates the effect of ionic strength on the interfacial tension and dilatational rheology of Gibbs monolayers of Pluronic F-68 solutions with different NaCl concentrations. This was made possible by combining several well-established experimental techniques that allowed us to evaluate the equilibrium isotherms and the interfacial dilational rheology of the formed monolayers. The results evidenced that the addition of salt significantly affects the interfacial tension while its impact on the dilational rheological response of the Pluronic F-68 Gibbs monolayers appears less important.

The effect of the ionic strength on the equilibrium isotherm is ascribed to a salting-out phenomenon that reduces the solubility of the hydrophilic blocks of the copolymer in the aqueous phase, enhancing its adsorption at the air/solution interface. This enhances the surface activity of Pluronic F-68, which results in a higher surface excess and stronger ability to lower the interfacial tension. However, this salting-out phenomenon, even though it is independent of the copolymer concentration, appears as a most important contribution to the surface activity of Pluronic F-68 when the NaCl concentration overcomes a threshold value around 1000 mM. The effect of such high concentrations of salt are rarely studied in works dealing with the adsorption of surface-active molecules at fluid interfaces.

On the contrary to that what was found for the impact of the ionic strength on the equilibrium properties of the Gibbs monolayers, the results obtained by low-frequency oscillatory experiments showed that the ionic strength has only a reduced effect on the modification of the relaxation processes, modifying the characteristic frequencies in such a way that can be interpreted in terms of the enhanced surface activity induced by the addition of salt. However, the extension of the accessible frequency range by including results obtained using measurements based on the evaluation of the damping of interfacial capillary waves excited by the application of an electric field evidenced that the rheological response of the Gibbs monolayers can be modified by the ionic strength, especially at high copolymer concentrations and high ionic strength. However, most interesting is the fact that the variation in the ionic strength and the copolymer bulk concentration helps in understanding of the limits of the characterization of interfacial rheology by electrocapillary wave experiments. The results have evidenced that these limits are not only a result of the surface excess and interfacial tension and deserve a deeper study to exploit the whole potential of electrocapillary waves for evaluating the dilational rheology properties of interfacial films at the air/water interface.

## Appendix A  Bulk Viscosity, Density, and Interfacial Tension

Table 1 reports the salt concentration dependence of the bulk viscosity, η, obtained using a capillary viscometer (Ubbelohde) and the bibliographic densities [61] and interfacial tensions [62] for aqueous NaCl solutions.

It should be noted that the addition of Pluronic F-68 to salty water does not provoke any significant modification in the bulk viscosity in relation to that of aqueous NaCl solutions. For instance, the bulk viscosity of a solution of Pluronic F-68 with concentration $= 10^{-1}$ mM and a NaCl concentration of 3000 mM was about 1.3 mPa·s, which is equivalent to that obtained for a NaCl solution of the same concentration. In the case of the density, a strong change in the density is not expected in relation to NaCl solutions for the diluted solutions studied in this work (Pluronic F-68 bulk density assumes a value of about 1.06 g/cm$^3$).

**Table A1.** Viscosity $\eta$ and density $\rho$ of aqueous NaCl solutions at 23 °C.

| NaCl [mM] | $\eta$ (mPa·s) | $\rho$ (g/cm$^3$) [1] | $\gamma$ (mN/m) [2] |
|---|---|---|---|
| 0 | 0.90 ± 0.03 | 0.998 | 72.72 |
| 100 | 0.91 ± 0.03 | 1.002 | - |
| 1000 | 1.05 ± 0.03 | 1.038 | 73.77 |
| 2000 | 1.15 ± 0.03 | 1.075 | 74.94 |
| 3000 | 1.30 ± 0.03 | 1.111 | 76.61 |

[1] Data extracted from reference [61]. [2] Data extracted from reference [62].

## References

1. Jarak, I.; Varela, C.L.; Tavares Da Silva, E.; Roleira, F.F.M.; Veiga, F.; Figueiras, A. Pluronic-Based Nanovehicles: Recent Advances in Anticancer Therapeutic Applications. *Eur. J. Med. Chem.* **2020**, *206*, 112526. [CrossRef]
2. Shamma, R.N.; Sayed, R.H.; Madry, H.; El Sayed, N.S.; Cucchiarini, M. Triblock Copolymer Bioinks in Hydrogel Three-Dimensional Printing for Regenerative Medicine: A Focus on Pluronic F127. *Tissue Eng. Part B Rev.* **2022**, *28*, 451–463. [CrossRef]
3. Ganguly, R.; Kumar, S.; Kunwar, A.; Nath, S.; Sarma, H.D.; Tripathi, A.; Verma, G.; Chaudhari, D.P.; Aswal, V.K.; Melo, J.S. Structural and Therapeutic Properties of Curcumin Solubilized Pluronic F127 Micellar Solutions and Hydrogels. *J. Mol. Liq.* **2020**, *314*, 113591. [CrossRef]
4. Singla, P.; Garg, S.; McClements, J.; Jamieson, O.; Peeters, M.; Mahajan, R.K. Advances in the Therapeutic Delivery and Applications of Functionalized Pluronics: A Critical Review. *Adv. Colloid Interface Sci.* **2022**, *299*, 102563. [CrossRef] [PubMed]
5. Lucia, A.; Girard, C.; Fanucce, M.; Coviella, C.; Rubio, R.G.; Ortega, F.; Guzmán, E. Development of an Environmentally Friendly Larvicidal Formulation Based on Essential Oil Compound Blend to Control *Aedes aegypti* Larvae: Correlations between Physicochemical Properties and Insecticidal Activity. *ACS Sustain. Chem. Eng.* **2020**, *8*, 10995–11006. [CrossRef]
6. Kumar, S.S.; Harikrishnan, K.K.; Urmila, S.P.; Gauri, V.; Saritha, A.; Gangopadhyay, M. Comprehensive Review of Pluronic®Polymers of Different Shapes with Prominent Applications in Photodynamic Therapy. *Eur. Polym. J.* **2023**, *200*, 112534. [CrossRef]
7. Alexandridis, P. Poly(Ethylene Oxide)/Poly(Propylene Oxide) Block Copolymer Surfactants. *Curr. Opin. Colloid Interface Sci.* **1997**, *2*, 478–489. [CrossRef]
8. Li, Z.; Peng, S.; Chen, X.; Zhu, Y.; Zou, L.; Liu, W.; Liu, C. Pluronics Modified Liposomes for Curcumin Encapsulation: Sustained Release, Stability and Bioaccessibility. *Food Res. Int.* **2018**, *108*, 246–253. [CrossRef] [PubMed]
9. Braga, G.; Campanholi, K.D.S.S.; Ferreira, S.B.D.S.; Calori, I.R.; De Oliveira, J.H.; Vanzin, D.; Bruschi, M.L.; Pontes, R.M.; Março, P.H.; Tessaro, A.L.; et al. Tautomeric and Aggregational Dynamics of Curcumin-Supersaturated Pluronic Nanocarriers. *ACS Appl. Polym. Mater.* **2020**, *2*, 4493–4511. [CrossRef]
10. Shaker, M.A.; Elbadawy, H.M.; Shaker, M.A. Improved Solubility, Dissolution, and Oral Bioavailability for Atorvastatin-Pluronic® Solid Dispersions. *Int. J. Pharm.* **2020**, *574*, 118891. [CrossRef]
11. Carbone, C.; Rubio-Bueno, A.; Ortega, F.; Rubio, R.G.; Guzmán, E. Adsorption of Mixed Dispersions of Silica Nanoparticles and an Amphiphilic Triblock Copolymer at the Water–Vapor Interface. *Appl. Sci.* **2023**, *13*, 10093. [CrossRef]
12. Velasco-Rodriguez, B.; Soltero-Martínez, J.F.; Rosales-Rivera, L.C.; Macías-Balleza, E.R.; Landázuri, G.; Larios-Durán, E.R. Adsorption and Interaction of Bovine Serum Albumin and Pluronic P103 Triblock Copolymer on a Gold Electrode: Double-Layer Capacitance Measurements. *ACS Omega* **2020**, *5*, 17347–17355. [CrossRef]
13. Yun, K.H.; Sharma, K.; Kim, H.U.; Bae, T.-H. Modification of a PES Microfiltration Membrane to Enhance Sterile Filtration by Inhibiting Protein Adsorption. *J. Ind. Eng. Chem.* **2023**, *123*, 311–319. [CrossRef]
14. Pérez-Sánchez, G.; Vicente, F.A.; Schaeffer, N.; Cardoso, I.S.; Ventura, S.P.M.; Jorge, M.; Coutinho, J.A.P. Rationalizing the Phase Behavior of Triblock Copolymers through Experiments and Molecular Simulations. *J. Phys. Chem. C* **2019**, *123*, 21224–21236. [CrossRef]
15. Hopkins, C.C.; De Bruyn, J.R. Gelation and Long-Time Relaxation of Aqueous Solutions of Pluronic F127. *J. Rheol.* **2019**, *63*, 191–201. [CrossRef]
16. Patel, D.; Jana, R.; Lin, M.-H.; Kuperkar, K.; Seth, D.; Chen, L.-J.; Bahadur, P. Revisiting the Salt-Triggered Self-Assembly in Very Hydrophilic Triblock Copolymer Pluronic®F88 Using Multitechnique Approach. *Colloid Polym. Sci.* **2021**, *299*, 1113–1126. [CrossRef]
17. Da Silva, L.H.M.; Loh, W. Calorimetric Investigation of the Formation of Aqueous Two-Phase Systems in Ternary Mixtures of Water, Poly(Ethylene Oxide) and Electrolytes (Or Dextran). *J. Phys. Chem. B* **2000**, *104*, 10069–10073. [CrossRef]
18. Suman, K.; Sourav, S.; Joshi, Y.M. Rheological Signatures of Gel–Glass Transition and a Revised Phase Diagram of an Aqueous Triblock Copolymer Solution of Pluronic F127. *Phys. Fluids* **2021**, *33*, 073610. [CrossRef]
19. Boonrat, O.; Tantishaiyakul, V.; Hirun, N.; Rugmai, S.; Soontaranon, S. Structural Characterization Using SAXS and Rheological Behaviors of Pluronic F127 and Methylcellulose Blends. *Polym. Bull.* **2021**, *78*, 1175–1187. [CrossRef]
20. Zheng, L.; Minamikawa, H.; Harada, K.; Inoue, T.; Chernik, G.G. Effect of Inorganic Salts on the Phase Behavior of an Aqueous Mixture of Heptaethylene Glycol Dodecyl Ether. *Langmuir* **2003**, *19*, 10487–10494. [CrossRef]

21. Pandit, N.; Trygstad, T.; Croy, S.; Bohorquez, M.; Koch, C. Effect of Salts on the Micellization, Clouding, and Solubilization Behavior of Pluronic F127 Solutions. *J. Colloid Interface Sci.* **2000**, *222*, 213–220. [CrossRef]

22. Sheelarani, B.; Karunanithi, P.; Dash, S. Effect of Valency of Cation on Micellization Behaviour of Pluronic Mixed Micelle F127 and L64. *Chem. Phys. Lett.* **2020**, *739*, 136956. [CrossRef]

23. Tripathi, N.; Ray, D.; Aswal, V.K.; Kuperkar, K.; Bahadur, P. Salt Induced Micellization Conduct in PEO–PPO–PEO-Based Block Copolymers: A Thermo-Responsive Approach. *Soft Matter* **2023**, *19*, 7227–7244. [CrossRef]

24. Rudani, B.A.; Sarolia, J.; Rai, R.; Aswal, V.K.; Bahadur, P.; Tiwari, S. Comparative Effect of Physiological Salts upon Micellization of T1304 and T1307. *Langmuir* **2023**, *39*, 9060–9068. [CrossRef]

25. Alexandridis, P.; Holzwarth, J.F. Differential Scanning Calorimetry Investigation of the Effect of Salts on Aqueous Solution Properties of an Amphiphilic Block Copolymer (Poloxamer). *Langmuir* **1997**, *13*, 6074–6082. [CrossRef]

26. Ward, C.L.; Cornejo, M.A.; Peli Thanthri, S.H.; Linz, T.H. A Review of Electrophoretic Separations in Temperature-Responsive Pluronic Thermal Gels. *Anal. Chim. Acta* **2023**, *1276*, 341613. [CrossRef] [PubMed]

27. Xu, L.; Li, X.; Zhai, M.; Huang, L.; Peng, J.; Li, J.; Wei, G. Ion-Specific Swelling of Poly(Styrene Sulfonic Acid) Hydrogel. *J. Phys. Chem. B* **2007**, *111*, 3391–3397. [CrossRef] [PubMed]

28. Loh, W.W.; Lin, Q.; Lim, C.C.; Guo, L.; Tang, Y.K.; Loh, X.J.; Lim, J.Y.C. Hofmeister Effects of Anions on Self-Assembled Thermogels. *Mater. Today Chem.* **2022**, *23*, 100674. [CrossRef]

29. Smith, J.D.; Saykally, R.J.; Geissler, P.L. The Effects of Dissolved Halide Anions on Hydrogen Bonding in Liquid Water. *J. Am. Chem. Soc.* **2007**, *129*, 13847–13856. [CrossRef] [PubMed]

30. Guàrdia, E.; Laria, D.; Martí, J. Hydrogen Bond Structure and Dynamics in Aqueous Electrolytes at Ambient and Supercritical Conditions. *J. Phys. Chem. B* **2006**, *110*, 6332–6338. [CrossRef]

31. Chen, X.; Flores, S.C.; Lim, S.-M.; Zhang, Y.; Yang, T.; Kherb, J.; Cremer, P.S. Specific Anion Effects on Water Structure Adjacent to Protein Monolayers. *Langmuir* **2010**, *26*, 16447–16454. [CrossRef] [PubMed]

32. Kontogiannis, O.; Selianitis, D.; Lagopati, N.; Pippa, N.; Pispas, S.; Gazouli, M. Surfactant and Block Copolymer Nanostructures: From Design and Development to Nanomedicine Preclinical Studies. *Pharmaceutics* **2023**, *15*, 501. [CrossRef]

33. Li, Y.; Tian, Y.; Jia, X.; Zhang, Z.; Sun, D.; Xie, H.; Zang, D.; Liu, T. Effect of Pharmaceutical Excipients on Micellization of Pluronic and the Application as Drug Carrier to Reverse MDR. *J. Mol. Liq.* **2023**, *383*, 122182. [CrossRef]

34. Deyerle, B.A.; Zhang, Y. Effects of Hofmeister Anions on the Aggregation Behavior of PEO–PPO–PEO Triblock Copolymers. *Langmuir* **2011**, *27*, 9203–9210. [CrossRef] [PubMed]

35. Ren, C.; Tian, W.; Szleifer, I.; Ma, Y. Specific Salt Effects on Poly(Ethylene Oxide) Electrolyte Solutions. *Macromolecules* **2011**, *44*, 1719–1727. [CrossRef]

36. Llamas, S.; Mendoza, A.J.; Guzmán, E.; Ortega, F.; Rubio, R.G. Salt Effects on the Air/Solution Interfacial Properties of PEO-Containing Copolymers: Equilibrium, Adsorption Kinetics and Surface Rheological Behavior. *J. Colloid Interface Sci.* **2013**, *400*, 49–58. [CrossRef]

37. Noskov, B.A.; Lin, S.-Y.; Loglio, G.; Rubio, R.G.; Miller, R. Dilational Viscoelasticity of PEO–PPO–PEO Triblock Copolymer Films at the Air–Water Interface in the Range of High Surface Pressures. *Langmuir* **2006**, *22*, 2647–2652. [CrossRef]

38. Rivillon, S.; Muñoz, M.G.; Monroy, F.; Ortega, F.; Rubio, R.G. Experimental Study of the Dynamic Properties of Monolayers of PS–PEO Block Copolymers: The Attractive Monomer Surface Case. *Macromolecules* **2003**, *36*, 4068–4077. [CrossRef]

39. Brinkkötter, M.; Geisler, R.; Großkopf, S.; Hellweg, T.; Schönhoff, M. Influence of Li-Salt on the Mesophases of Pluronic Block Copolymers in Ionic Liquid. *J. Phys. Chem. B* **2020**, *124*, 9464–9474. [CrossRef]

40. Kumar, Y.; Hashmi, S.A.; Pandey, G.P. Lithium Ion Transport and Ion–Polymer Interaction in PEO Based Polymer Electrolyte Plasticized with Ionic Liquid. *Solid State Ion.* **2011**, *201*, 73–80. [CrossRef]

41. Li, X.; Huang, K.; Xu, Y.; Liu, H. Interaction of Sodium and Potassium Ions with PEO-PPO Copolymer Investigated by FTIR, Raman and NMR. *Vib. Spectrosc.* **2014**, *75*, 59–64. [CrossRef]

42. Díez-Pascual, A.M.; Monroy, F.; Ortega, F.; Rubio, R.G.; Miller, R.; Noskov, B.A. Adsorption of Water-Soluble Polymers with Surfactant Character. Dilational Viscoelasticity. *Langmuir* **2007**, *23*, 3802–3808. [CrossRef]

43. Cabrerizo-Vílchez, M.A.; Wege, H.A.; Holgado-Terriza, J.A.; Neumann, A.W. Axisymmetric Drop Shape Analysis as Penetration Langmuir Balance. *Rev. Sci. Instrum.* **1999**, *70*, 2438–2444. [CrossRef]

44. Torcello-Gómez, A.; Maldonado-Valderrama, J.; Gálvez-Ruiz, M.J.; Martín-Rodríguez, A.; Cabrerizo-Vílchez, M.A.; De Vicente, J. Surface Rheology of Sorbitan Tristearate and β-Lactoglobulin: Shear and Dilatational Behavior. *J. Non-Newton. Fluid Mech.* **2011**, *166*, 713–722. [CrossRef]

45. Berry, J.D.; Neeson, M.J.; Dagastine, R.R.; Chan, D.Y.C.; Tabor, R.F. Measurement of Surface and Interfacial Tension Using Pendant Drop Tensiometry. *J. Colloid Interface Sci.* **2015**, *454*, 226–237. [CrossRef]

46. Liggieri, L.; Santini, E.; Guzmán, E.; Maestro, A.; Ravera, F. Wide-Frequency Dilational Rheology Investigation of Mixed Silica Nanoparticle–CTAB Interfacial Layers. *Soft Matter* **2011**, *7*, 7699. [CrossRef]

47. Maestro, A.; Ortega, F.; Rubio, R.G.; Rubio, M.A.; Krägel, J.; Miller, R. Rheology of Poly(Methyl Methacrylate) Langmuir Monolayers: Percolation Transition to a Soft Glasslike System. *J. Chem. Phys.* **2011**, *134*, 104704. [CrossRef] [PubMed]

48. Monroy, F.; Ortega, F.; Rubio, R.G.; Velarde, M.G. Surface Rheology, Equilibrium and Dynamic Features at Interfaces, with Emphasis on Efficient Tools for Probing Polymer Dynamics at Interfaces. *Adv. Colloid Interface Sci.* **2007**, *134–135*, 175–189. [CrossRef] [PubMed]

49. Guzmán, E.; Maestro, A.; Carbone, C.; Ortega, F.; Rubio, R.G. Dilational Rheology of Fluid/Fluid Interfaces: Foundations and Tools. *Fluids* **2022**, *7*, 335. [CrossRef]

50. Ramírez, P.; Stocco, A.; Muñoz, J.; Miller, R. Interfacial Rheology and Conformations of Triblock Copolymers Adsorbed onto the Water–Oil Interface. *J. Colloid Interface Sci.* **2012**, *378*, 135–143. [CrossRef] [PubMed]

51. Torcello-Gómez, A.; Santander-Ortega, M.J.; Peula-García, J.M.; Maldonado-Valderrama, J.; Gálvez-Ruiz, M.J.; Ortega-Vinuesa, J.L.; Martín-Rodríguez, A. Adsorption of Antibody onto Pluronic F68-Covered Nanoparticles: Link with Surface Properties. *Soft Matter* **2011**, *7*, 8450–8461. [CrossRef]

52. Alexandridis, P.; Athanassiou, V.; Fukuda, S.; Hatton, T.A. Surface Activity of Poly(Ethylene Oxide)-Block-Poly(Propylene Oxide)-Block-Poly(Ethylene Oxide) Copolymers. *Langmuir* **1994**, *10*, 2604–2612. [CrossRef]

53. Alexandridis, P.; Holzwarth, J.F.; Hatton, T.A. Micellization of Poly(Ethylene Oxide)-Poly(Propylene Oxide)-Poly(Ethylene Oxide) Triblock Copolymers in Aqueous Solutions: Thermodynamics of Copolymer Association. *Macromolecules* **1994**, *27*, 2414–2425. [CrossRef]

54. Muñoz, M.G.; Monroy, F.; Hernández, P.; Ortega, F.; Rubio, R.G.; Langevin, D. Anomalous Damping of the Capillary Waves at the Air–Water Interface of a Soluble Triblock Copolymer. *Langmuir* **2003**, *19*, 2147–2154. [CrossRef]

55. Jeworrek, C.; Evers, F.; Howe, J.; Brandenburg, K.; Tolan, M.; Winter, R. Effects of Specific versus Nonspecific Ionic Interactions on the Structure and Lateral Organization of Lipopolysaccharides. *Biophys. J.* **2011**, *100*, 2169–2177. [CrossRef]

56. Lucassen, J.; Van Den Tempel, M. Dynamic Measurements of Dilational Properties of a Liquid Interface. *Chem. Eng. Sci.* **1972**, *27*, 1283–1291. [CrossRef]

57. Langevin, D. *Light Scattering by Liquid Surfaces and Complementary Techniques*; Surfactant Science Series; Marcel Dekker: New York, NY, USA, 1992; ISBN 978-0-8247-8607-6.

58. Levich, V.G. *Physicochemical Hydrodynamics*, 2nd ed.; Prentice-Hall: Englewood Cliffs, NJ, USA, 1962; ISBN 978-0-13-674440-5.

59. Lucassen-Reynders, E.H.; Lucassen, J. Properties of Capillary Waves. *Adv. Colloid Interface Sci.* **1970**, *2*, 347–395. [CrossRef]

60. Ravera, F.; Ferrari, M.; Santini, E.; Liggieri, L. Influence of Surface Processes on the Dilational Visco-Elasticity of Surfactant Solutions. *Adv. Colloid Interface Sci.* **2005**, *117*, 75–100. [CrossRef] [PubMed]

61. Lide, D.R. (Ed.) *CRC Handbook of Chemistry and Physics: A Ready-Reference Book of Chemical and Physical Data*, 79th ed.; CRC: Boca Raton, FL, USA, 1998; ISBN 978-0-8493-0479-8.

62. Ozdemir, O.; Karakashev, S.I.; Nguyen, A.V.; Miller, J.D. Adsorption and Surface Tension Analysis of Concentrated Alkali Halide Brine Solutions. *Miner. Eng.* **2009**, *22*, 263–271. [CrossRef]